



Griggs, J. A., & Harries, J. E. (2005). Comparison of spectrally resolved outgoing longwave radiation between 1970 and 2003: The 4 band of methane. *Proceedings of SPIE*, 5883. DOI: 10.1117/12.621607

Peer reviewed version

Link to published version (if available):
[10.1117/12.621607](https://doi.org/10.1117/12.621607)

[Link to publication record in Explore Bristol Research](#)
PDF-document

University of Bristol - Explore Bristol Research

General rights

This document is made available in accordance with publisher policies. Please cite only the published version using the reference above. Full terms of use are available:
<http://www.bristol.ac.uk/pure/about/ebr-terms>

Comparison of spectrally resolved outgoing longwave radiation between 1970 and 2003: The ν_4 band of methane

Jennifer A. Griggs^a and John E. Harries^b

^aImperial College London, Prince Consort Road, London, United Kingdom, now at Bristol
Glaciology Centre, University of Bristol, Bristol, United Kingdom

^bImperial College London, Prince Consort Road, London, United Kingdom

ABSTRACT

Measurements of spectrally resolved outgoing longwave radiation recorded in 1970, 1997 and 2003 are compared to determine the change in radiative forcing over that period. The changes are shown to be in agreement with that simulated by MODTRAN, a band model, using the known changes in atmospheric temperature and greenhouse gas concentrations when the effects of noise in the observed spectra are considered. The only region where the simulations are unable to reproduce the observations is in the ν_4 band of methane around 1306cm^{-1} . The methane profiles used to simulate this region of the spectrum are shown to be in good agreement with all available data and the noise levels on the spectra are small. Therefore, it is proposed that the inability to model this region lies in the model formulation. Genln2, a line-by-line model, is shown to give very different results in this particular band to those obtained using MODTRAN. Sensitivity studies show that Genln2 is also not able to fully reproduce the spectrum observed. Errors in the spectroscopic parameters are shown to be smaller than the observed discrepancy and line mixing in methane is suggested as a possible cause of the discrepancy.

Keywords: outgoing longwave radiation, spectrum, greenhouse gases, simulation, infrared, methane, HITRAN

1. INTRODUCTION

The Earth's climate system has been extensively studied and strong evidence exists linking surface temperatures and greenhouse gas concentrations. The spectrally resolved outgoing longwave radiation (OLR) is a measure of the cooling of the atmosphere to space and as such exhibits signatures which are characteristic of surface properties as well as absorption and emission by greenhouse gases in the atmosphere. Comparison of spectrally resolved OLR datasets allows a detection of the multiple components of the radiative forcing on the atmosphere simultaneously. No long term records of spectrally resolved OLR exist and so a comparison is complicated by the need to firstly normalise datasets from instruments with differing specifications to the specifications of one dataset. The first such comparison of spectrally resolved OLR recorded in 1970 and 1997 was presented in Harries et al.¹ The initial results of a follow-up analysis including new data from 2003 was then presented by Griggs and Harries.² In this paper, we recap on the previous results and discuss, in detail, our ability to simulate to observed spectrally resolved OLR in one particular absorption band, the ν_4 band of methane. The focus on this band is necessitated by the inability to accurately simulate this band. To begin, we discuss the three datasets compared and present the observed and simulated comparisons of spectrally resolved OLR. We then discuss our ability of simulate the spectrally resolved OLR in the ν_4 band of methane and suggest possible improvements.

2. DATA

The data used in this study were recorded by the IRIS (Infrared Interferometric Spectrometer),^{3,4} IMG (Interferometric Monitor for Greenhouse Gases)^{5,6} and AIRS (Atmospheric Infrared Sounder)⁷ instruments. The pertinent properties of the IRIS, IMG and AIRS instruments are listed in table 1 with the details presented below. The main time period of overlapping data is the months of April, May and June and this time period is used throughout. The spectral range used is $700\text{-}1400\text{cm}^{-1}$ which is the maximum available when considering the high noise at low wavenumbers in the IMG spectra and high wavenumbers in the IRIS spectra.

Further author information:

E-mail: j.harries@imperial.ac.uk, Telephone: +44 (0) 207 59 47670

Table 1. Comparison of the properties of the IRIS, IMG and AIRS instruments.

Characteristic	IRIS	IMG	AIRS
Spectral Range (cm^{-1})	400-1600	600-3030	650-2700
Spatial Field of View	95x95km	8kmx8km	13.5kmx13.5km (nadir) 41kmx22.4km (zenith)
Spectral Resolution (cm^{-1})	2.8	0.10-0.25	0.4-1.0
Noise equivalent spectral radiance ($\text{mW m}^{-2}\text{sr}^{-1}$ per cm^{-1})	± 0.23	$\pm(0.31-0.6)$	$\pm(0.01-0.8)$

2.1. IRIS

The oldest instrument used in this study is the IRIS-D (Infrared Interferometric Spectrometer) instrument.^{3,4} IRIS-D (subsequently referred to as IRIS) flew on the NASA Nimbus 4 satellite which was launched in April 1970 into an 1100km altitude sun-synchronous polar orbit. It recorded data until January 1971 when it was switched off having fulfilled its design brief. IRIS was a Fourier transform spectrometer (FTS) and for its time was considered highly adventurous in its aims. It recorded spectra between 400cm^{-1} and 1600cm^{-1} but wavenumbers over 1400cm^{-1} suffer from high noise. Its field of view allowed it to record spectra with a ground footprint of 95km diameter and it had an apodized spectral resolution of 2.8cm^{-1} . All aspects of the design of IRIS represented a large leap in the design of FTS' particularly the high resolution and wide spectral range combined with an instrument small and resilient enough to be spaceborne.

2.2. IMG

IMG (Interferometric Monitor for Greenhouse Gases)^{5,6} was a much more advanced FTS. It was launched in August 1996 onboard the ADEOS satellite. Data was recorded between November 1996 and June 1997 when operations ceased as a result of satellite failure. IMG had a spectral resolution of 0.1cm^{-1} and a spectral range of $600-3030\text{cm}^{-1}$. To ensure that the smooth movement of the mirror and optical alignment were maintained, the mirror movement system was designed using a magnetic suspension system. As the instrument was required to have a wide spectral range, one detector could not cover the entire range. Three different detectors were required, each recording a different part of the spectrum. The only detector used in this study recorded between 600 and 2000cm^{-1} . Data are only usable at wavenumbers larger than 700cm^{-1} due to noise in the lower wavenumber section. ADEOS orbited in a 797km altitude polar sun-synchronous orbit giving a square ground footprint of 8km by 8km. Except for a 10 day period between 1st and 10th April when the instrument recorded continuously, IMG operated in a 4 day on, 10 day off cycle. At the start of routine operations in November 1996, it was discovered that the moving mirror alignment system was sticking randomly causing unacceptable degradation in the quality of the spectrum being recorded at the time. Tests were ongoing to try and adjust the gain system to compensate for this effect when the satellite failed. The problems caused 85% of the spectra recorded to be discarded as being unacceptably noisy.

2.3. AIRS

The Atmospheric Infrared Sounder (AIRS)⁷ was launched on the EOS-Aqua satellite in May 2002. AIRS is a grating spectrometer rather than the FTS design of the previous two instruments. It uses this design to achieve similar resolution and spectral range to IMG but at a much greater speed, enabling far greater coverage than that achieved by either IRIS or IMG. The spectral range of AIRS is from 650cm^{-1} to 2700cm^{-1} measured by 2378 channels which are separated into 17 modules of detectors which do not overlap, resulting in non-contiguous spectral coverage. Eight gaps occur in the $700-1400\text{cm}^{-1}$ spectral range considered in this study. Each channel has at least two times redundancy on the detectors but 238 channels are present which either have failed or are too noisy to use in the 700cm^{-1} to 1400cm^{-1} region. These channels are simply interpolated over in the analysis except in the 1226cm^{-1} and 1347cm^{-1} regions where multiple neighbouring channels failed and additional spectral gaps had to be created. The spectral resolution of a grating spectrometer is controlled by the aperture of the detectors on the focal plane array of the instrument. The detectors in AIRS are all $10\mu\text{m}$ by $10\mu\text{m}$

squares with $10\mu\text{m}$ gaps between each detector and its nearest neighbour giving a resolution of between 0.4cm^{-1} and 1cm^{-1} .

The recording geometry of AIRS is very different to that of the other two instruments. IRIS views nadir through a fixed aperture and image compensation mirror. The detector arrangement of the IMG instrument means that two of the three detectors must view the Earth from very slightly off-nadir. The detector recording the data used here is one of these slightly off-nadir viewing detectors. To enhance the spatial coverage and to take advantage of its speed, AIRS scans to $\pm 49.5^\circ$ cross track as the satellite moves forwards taking 90 spectra each with an instantaneous field of view of 1.1° in a row perpendicular to the direction of motion of the satellite. This results in a ground footprint of 13.5km diameter at nadir but closer to 41km by 22.4km at the largest zenith angles. Only the central eight spectra from each row of 90 are used in this study to ensure that off axis beams with longer atmospheric path lengths than that recorded by the IRIS instrument are not included.

3. COMPARISON METHOD

The comparison method used to normalise the three datasets to the specifications of IRIS is discussed in Griggs and Harries^{2, 8} and we will discuss only the most pertinent aspects here. The two properties of the spectrum which are normalised are the spectral resolution and the shift in wavenumber due to field of view effects in the FTS instruments. The normalisation is achieved in a two step process. Firstly, the resolution of IMG was lowered to that of AIRS by multiplying the IMG interferogram by an appropriately sized Hamming window. The interferograms are then re-transformed back to the spectral domain and shifted along the wavenumber scale to the unshifted position of the AIRS spectra.

The second stage of the normalisation process then reduced the resolution of the AIRS and AIRS resolution IMG spectra to the resolution of IRIS by convolving the spectra with the Fourier transform of an appropriately sized Hamming window. This different, but equivalent, smoothing process is necessary due to the gaps in the AIRS spectra. The, now IRIS resolution, AIRS and IMG spectra are then shifted along the wavenumber scale to the position of the IRIS spectra. At this point, the specifications of the three datasets are equivalent and comparison of these three datasets has been shown to be valid. The comparisons are all undertaken on cloud free, ocean based spectra due to the difficulty in attributing changes in average spectra recorded over a variety of land surfaces and the need for thorough coverage and good spectrally resolved cloud models to attribute changes in spectrally resolved OLR which include the effects of cloud. The cloud clearing process is achieved by a two step, sea surface temperature threshold and bispectral threshold technique as described in Griggs and Harries.^{2, 8}

4. OBSERVATIONAL SPECTRAL OLR DIFFERENCES

Differences are presented between spectra in the central Pacific region defined as 10°N - 10°S and 180°E - 230°E . Multiple regions have been examined showing consistent results.⁸ The cloud clearing process removes 99% of IRIS spectra, 67% of IMG spectra and 76% of AIRS spectra. The differing percentages are due to the differing fields of view of the three instruments and thus the differing probability of viewing between broken cloud. The average spectra from each instrument and the differences between those spectra in the central Pacific in April, May and June are shown in figure 1. The average spectrum for each instrument for the central Pacific region is shown in figure 1(a) showing consistent width and wavenumber of individual absorption features in spectra from all instruments. This indicates that the resolution and field of view corrections have been correctly applied. Figure 1(b) shows the differences between the average spectra shown in figure 1(a). The lower line is the 1997 IMG spectrum minus the 1970 IRIS spectrum; the middle line is the 2003 AIRS spectrum minus the 1970 IRIS spectrum; and the upper line is the 2003 AIRS spectrum minus the 1997 IMG spectrum. Offsets of -5K and -10K have been applied to the AIRS-IRIS (2003-1970) and IMG-IRIS (1997-1970) difference spectra respectively to aid the clarity of the plot. In all cases, the difference spectra are seen to have consistent and reproducible features, an indication that changes in the atmospheric conditions may be producing consistent signals which can be observed and attributed. Figures 1(c), (d) and (e) show the individual difference spectra with the standard errors on the difference indicated by the thickness of the line. The vertical grey shading in the three figures shows the regions of the spectrum which are significantly different from zero at the 95% confidence level. The statistical significance of the majority of the difference spectra is an indication that both the temporal and spatial sampling is adequate.

Features are seen in the areas of the spectrum where the absorption bands of a number of the major greenhouse gases occur. Features are observed in the water vapour lines in the 1200 - 1400cm^{-1} region, the ozone ν_3 band around 1060cm^{-1} ,

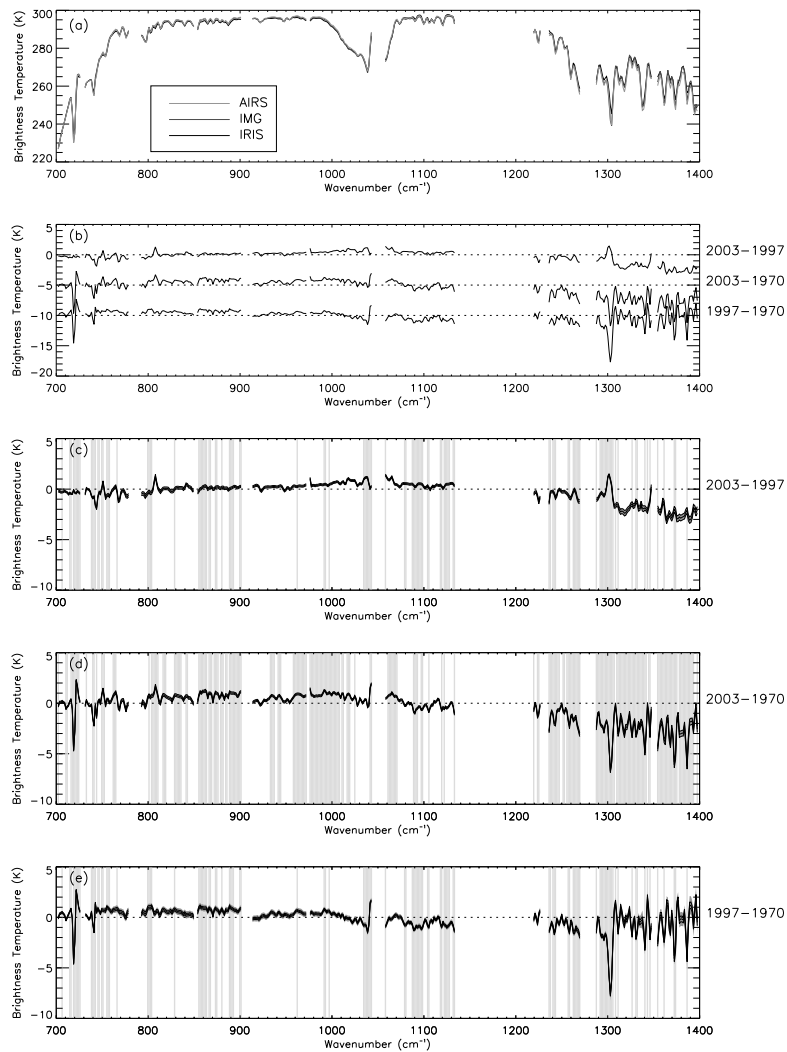


Figure 1. The average spectrum from each instrument and the differences between them in the central Pacific region in April, May and June. Figure (a) shows the average spectrum from each instrument. Figure (b) shows the differences between the average spectra from the three instruments. The upper line is the AIRS-IMG (2003-1997) spectrum, the middle line is the AIRS-IRIS (2003-1970) spectrum offset by -5K and the lower line is the IMG-IRIS (1997-1970) spectrum offset by -10K. The offsets are purely for the clarity of the plot. Figure (c) again shows the AIRS-IMG (2003-1997) difference spectrum, figure (d) shows the AIRS-IRIS (2003-1970) difference spectrum and figure (e) shows the IMG-IRIS (1997-1970) difference spectrum. Figures (c), (d) and (e) all present the standard error on the difference spectrum as the thickness of the line and the regions of the difference spectrum with 95% statistical significance that the differences shown are non-zero are those areas which are shaded with vertical light grey lines.

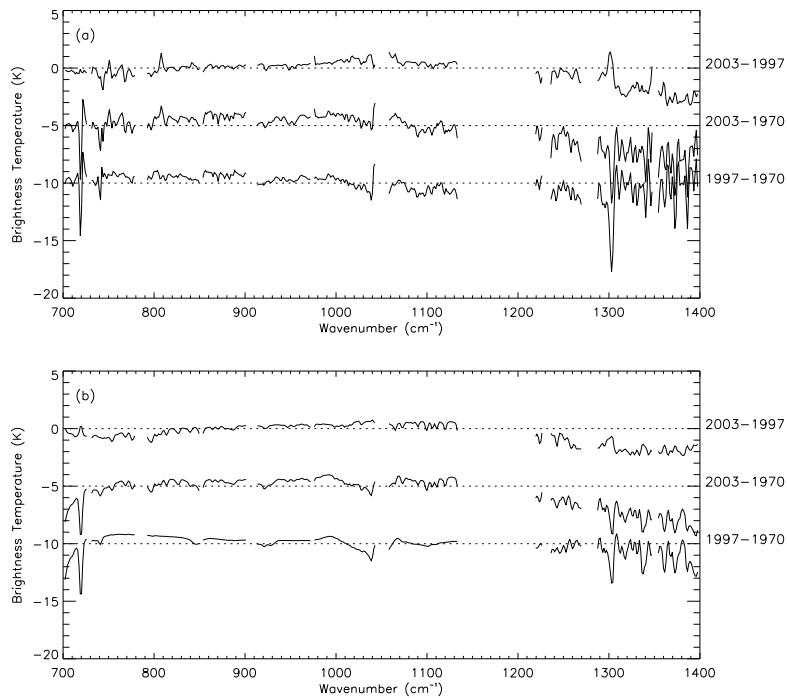


Figure 2. The simulated difference spectra created using the ‘optimised’ gas concentration and temperature profiles. Figure (a) shows the observed difference spectra as shown in figure 1(b). Figure (b) shows the best achievable simulation of the observed difference spectrum.

the carbon dioxide ν_2 band at 700cm^{-1} and the methane ν_4 band close to 1300cm^{-1} . An interesting and unique feature is observed in the methane band of the three difference spectra. In the AIRS-IRIS and IMG-IRIS difference spectra, a negative going brightness temperature difference is observed indicating either an increase in methane, in line with the observed surface concentration of methane, or a large decrease in atmospheric temperature. In the AIRS-IMG difference spectra, showing the change over the last 8 years, a positive going brightness temperature difference is observed. This indicates either a decrease in methane concentration or an increase in atmospheric temperature. The surface record of methane concentrations,⁹ albeit not a record which is well sampled spatially, indicates that methane has increased slightly over the same period. The increase in atmospheric temperature is the more probable cause of the positive going brightness temperature observed.

Figure 2 shows the best simulation of the observed differences. The spectra were simulated using the MODTRAN4 model¹⁰ with spectroscopic parameters taken from the Hitran 2000 database with updates to 2001.¹¹ The profiles used in the simulation were determined iteratively by considering any profiles with physically realistic gradients with concentrations between the maximum and minimum observed profiles. Details of the profiles used and a full explanation of the cause of the observed differences in spectrally resolved outgoing longwave radiation can be found in Griggs and Harries^{2, 8} where this simulation is referred to as the ‘best fit’ or ‘optimised’ simulation. If the combined noise equivalent brightness temperature on the difference spectra is considered, with the exception of the region of spectra dominated by the absorption and emission by ν_4 band of methane, the observed difference spectra agree with that simulated using the known changes in greenhouse gas concentrations and atmospheric temperatures. The case of the methane band is unique in the spectrum, being the only region of the spectrum which, both in this study and in Harries et al.,¹ can not be simulated using the known changes in methane, water vapour concentration and atmospheric temperature. In the remainder of this study, we focus on the region of the spectrum dominated by the absorption and emission by ν_4 band of methane.

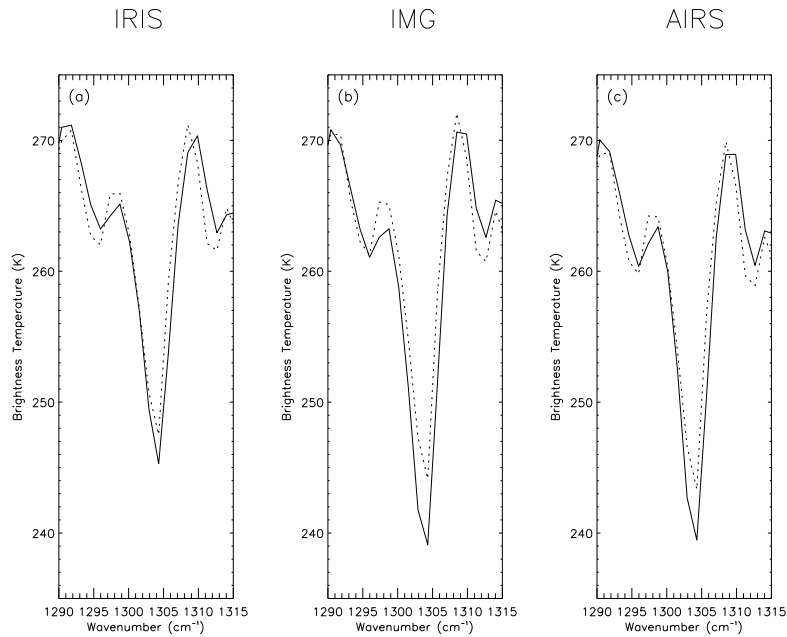


Figure 3. Figures (a), (b) and (c) show the observed (solid line) and simulated (dotted line) spectrum in the region of the spectrum dominated by the effects of methane for 1970, 1997 and 2003 respectively.

5. METHANE BAND

We begin by discussing the profiles used in the simulation in figure 2 and the resulting simulation. Figure 3 the simulated and observed spectra in the $1295\text{-}1310\text{cm}^{-1}$ spectral region. The simulated spectra provide the best achievable match to the observations for the three years 1970, 1997 and 2003 in the methane band while maintaining the accurate simulation in the rest of the $700\text{-}1400\text{cm}^{-1}$ spectral range. It can be seen that the simulated methane band in all years (figures 3(a),(b) and (c)) has a higher brightness temperatures than that observed. In the remainder of this paper, the cause of this lack of depth is investigated. The focus is on the simulations of the years 1997 and 2003 both due to the better coverage of methane concentration measurements in those years than in 1970 and due to the interest in the positive going brightness temperature difference observed in the AIRS-IMG difference spectra (figure 1(c)).

The profiles of water vapour and temperature used to simulate the spectrum in the methane region in 1997 and 2003 were those which best simulated the entire $700\text{-}1400\text{cm}^{-1}$ spectral region. The methane profile used in the 1997 simulation (figure 3(b)) was the US tropical atmosphere¹² scaled by the single maximum methane concentration observed in the $10^{\circ}\text{N}\text{-}10^{\circ}\text{S}$ zonal band in the months of April, May and June by the CMDL ground flask analysis system (1.7ppmv). That used in the 2003 simulation (figure 3(c)) was the US tropical atmosphere scaled by a value of 1.785ppmv. This value was obtained by extrapolating the trend in the CMDL dataset from 2001 and estimating the maximum using the spread around the mean in the previous years. This extrapolation was used as, at the time of analysis, the CMDL data for 2003 were not available. These data have since become available and the maximum value is very close to that extrapolated (1.78ppmv observed, 1.785ppmv extrapolated).

To account for the differences between the simulated and observed spectra, the hypothesis that the US tropical atmosphere and the CMDL ground based flask analysis system can not adequately represent the profile observed is tested. Additional methane data are available from CMDL in-situ observatories,¹³ CMDL aircraft measurements made using the same system as the ground flask analysis and from HALOE¹⁴ as well as the CMDL ground flask analyses. In figure 4(a), all available data from the four sources from April, May and June 1997 between 45°N and 45°S in the entire zonal band is plotted as a box whisker plot. 45°N to 45°S is chosen so that aircraft data, which is only available for the higher latitudes and is the only data covering the lower to mid-troposphere can be included. Figure 4(b) shows the same data as figure 4(a) but for April, May and June 2003. It can be seen that the US tropical atmosphere scaled by the CMDL ground flask measurements is within the range of measurements from all sources particularly in the height range over 200hPa where

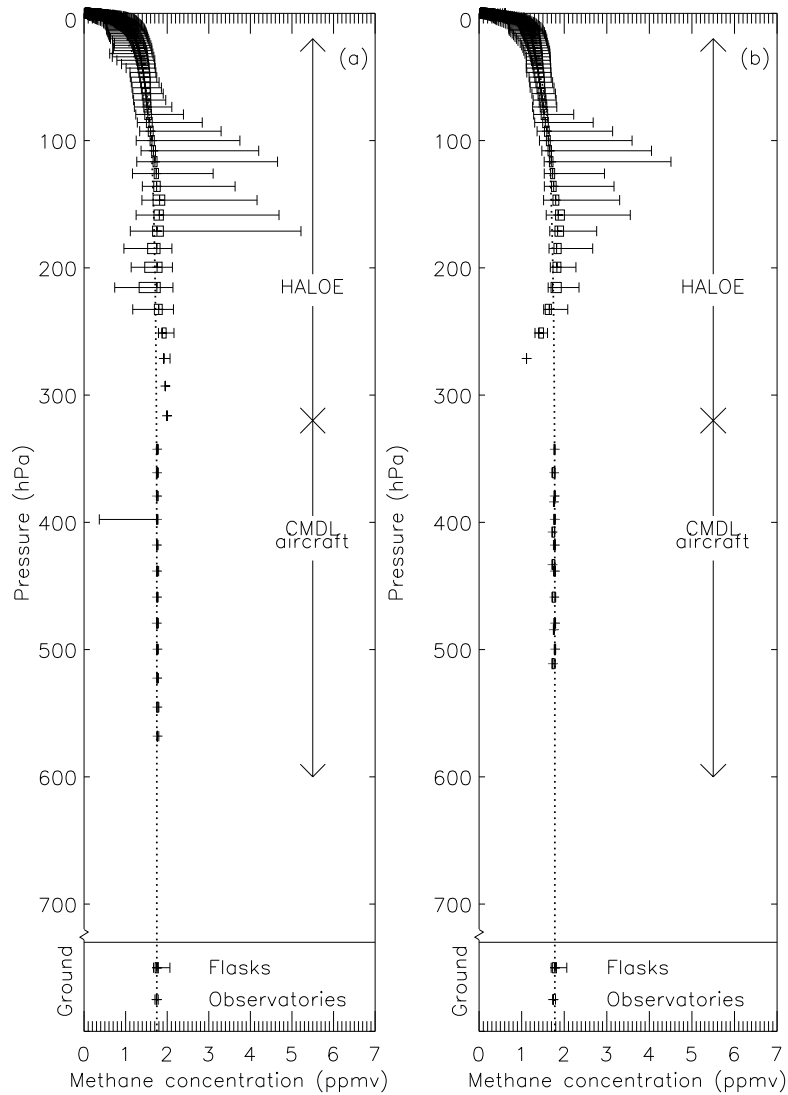


Figure 4. Box whisker plot of available CH_4 measurements. Figure (a) shows the available CH_4 measurements at all altitudes in April, May and June 1997 between 45°N and 45°S in the entire zonal band. Figure (b) as (a) but for April, May and June 2003. In the pressure range above 300hPa in both figures the measurements obtained by HALOE are shown. In the 700hPa to 300hPa range, the measurements obtained by the CMDL aircraft are shown. At ground level, both the measurements from the CMDL ground flask analysis and the CMDL in-situ observatories are plotted. At each height where concentration data exists, the data is shown as a cross for the median observation, a box outline the 25th to 75th percentiles and a horizontal lines showing the maximum and minimum values observed.

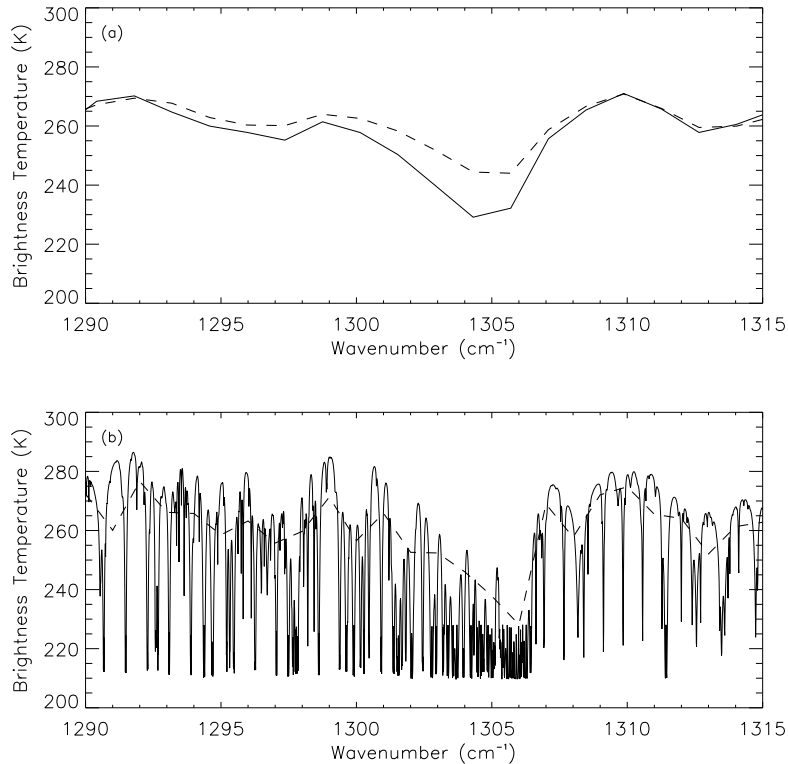


Figure 5. Comparison of 1290-1315cm⁻¹ region as simulated by MODTRAN and Genln2. In both simulations, the input profiles are those used in the 2003 optimised simulation and identical line shapes and spectroscopy are used. Figure (a) shows the simulation created using the Genln2 (solid line) and MODTRAN (dashed line) radiative transfer models, both smoothed to the 2.8cm⁻¹ IRIS resolution. Figure (b) shows the two simulations at their original unsmoothed resolutions of 0.01cm⁻¹ for Genln2 (solid line) and 1cm⁻¹ for MODTRAN (dashed line).

the spectrum is most sensitive to the effects of methane. This shows that the methane profiles used in the simulations are representative of the full profiles observed.

The other possible cause of the inability to simulate this region of the spectrum is the model formulation. It has been shown, by ourselves and Theriault et al,¹⁵ that, when examining differences between spectra, results from a band model are essentially equivalent to those achieved using a line-by-line model. When difference spectra are simulated using MODTRAN and Genln2,¹⁶ a line-by-line model, with identical input profiles and spectroscopic parameters specified, small discrepancies between the spectra simulated by the two models can be seen. The maximum difference between the two models is in the methane band and is around 1K for the IMG-IRIS difference spectrum. This is much less than the difference between the observed and MODTRAN simulated spectra. However, when examining the simulated spectra, rather than the differences between them, major differences between the two modelling methodologies are seen. Figure 5(a) shows the simulation of the methane band created using both MODTRAN (dashed line) and Genln2 (solid line) smoothed to the 2.8cm⁻¹ resolution used throughout this study. Genln2 clearly simulated a much stronger absorption band for the same methane concentrations. Figure 5(b) shows the equivalent simulation for both MODTRAN and Genln2 at their original resolutions of, respectively, 1cm⁻¹ and 0.01cm⁻¹. It is seen that the finely spaced lines of the Q branch are not well reproduced by MODTRAN particularly between 1302cm⁻¹ and 1306cm⁻¹.

The outstanding question now remains, can Genln2 accurately simulate the spectra recorded by IRIS, IMG and AIRS in the region dominated by absorption and emission by methane? A complete rerun of the iteration process used in section 4 is not practical with Genln2, therefore an initial sensitivity study is performed. Here, simulations are created using the maximum and minimum observed temperature, water vapour and methane concentrations for the three month period to determine whether the observed spectra lie within the range of these outlying simulations. This will determine whether a

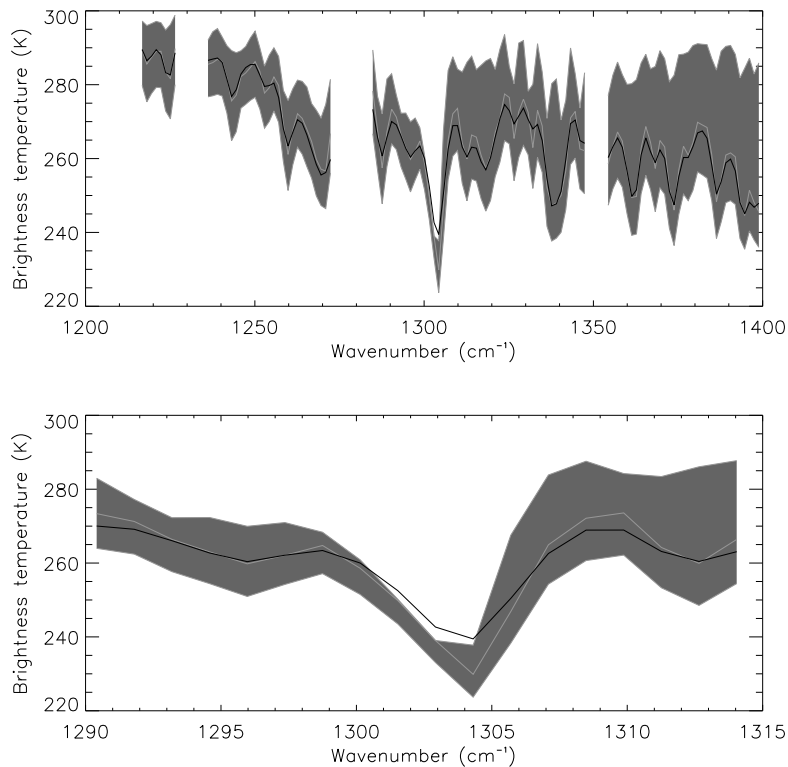


Figure 6. Sensitivity study into the combined effect of the maximum and minimum observed water vapour, temperature and methane concentrations on the simulated spectrum in the central Pacific in April, May and June 2003. The thickness of the shaded band indicates the range of possible simulations bounded at the higher brightness temperature end by the simulation including the highest temperature, lowest water vapour concentration and lowest methane concentration observed and at the lower brightness temperature end by the simulation including the lowest temperature, highest water vapour concentration and highest methane concentration. The central white line shows the simulation with the average water vapour concentration and temperature profiles and the modal methane concentration for the central Pacific in April, May and June. The black line shows the observed average spectrum in the central Pacific. Figure (a) shows the $1200\text{-}1400\text{cm}^{-1}$ region of the spectrum and (b) shows the $1290\text{-}1315\text{cm}^{-1}$ region of emission by methane.

reiteration using GenIn2 will be able to produce an accurate simulation of the methane band.

The resulting spectra are shown in figure 6. In both panels, the width of the grey shaded band shows the ranges of simulations which could be achieved. In all cases, the maximum and minimum water vapour concentrations and temperatures are the maximum and minimum values in the central Pacific region in April, May and June 2003 in the NCEP reanalysis datasets. The range of methane profiles is obtained from the maximum and minimum CMDL ground flask sampling system concentrations scaled by the US tropical atmosphere. The methane concentrations are taken from the $10^{\circ}\text{N}\text{-}10^{\circ}\text{S}$ zonal band in April, May and June 2003. In both panels, the upper line is the simulation created using the maximum observed temperature, minimum observed water vapour concentration and minimum observed methane concentration. The lower line is the simulation created using the minimum observed temperature, maximum observed water vapour concentration and maximum observed methane concentration. The white central line is the simulation created using the average temperature, water vapour and methane concentrations. The dark line is the observed average spectrum in the central Pacific from April, May and June 2003. Figure 6(a) shows the $1200\text{-}1400\text{cm}^{-1}$ region. It is clear that, with the exception of the methane band, the observed spectrum lies well within the range of the simulated spectra and close to that simulated using the average profiles. In the methane band (figure 6(b)), the observed spectrum is at a higher brightness temperature than the range of the simulated spectra. It is interesting to note that, whilst MODTRAN was unable to simulate a deep enough methane band, GenIn2 is unable to simulate a shallow enough methane band.

It was previously determined that the US standard atmospheric profile and CMDL ground based flask analysis was a

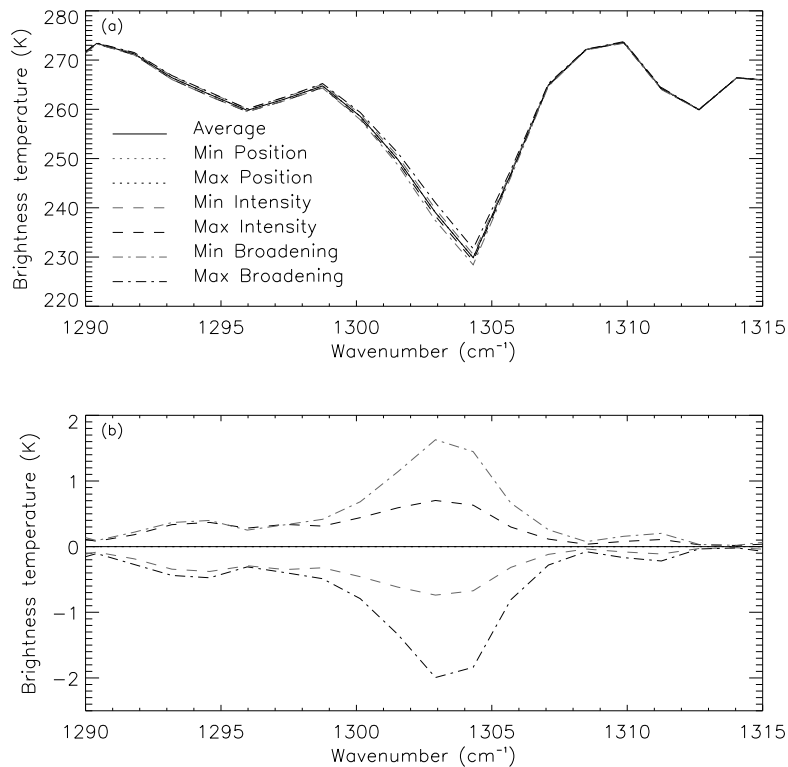


Figure 7. Simulated methane band using the range of uncertainty in the line position, intensity and air broadening half-width values in the 2001 updates to HITRAN2000. The solid black line shows a simulation of the central Pacific in April, May and June 2003 using the published values of line position, intensity and half-width. The gas concentrations are taken as follows: water vapour and temperature are average NCEP profiles, ozone is the average Hadley Centre model profile scaled by the average TOMS value and the other gases are the standard tropical atmosphere profiles scaled by the average CMDL ground flask gas concentration. The grey and black dotted lines show the average simulation with the line positions changed to the published values minus the known inaccuracies and plus the known inaccuracy respectively. The grey and black dashed lines show the average simulation with the line intensities increased and decreased by the maximum published inaccuracy respectively. The grey and black dot-dash lines show the average simulation with the air broadening half-widths increased and decreased by the maximum published inaccuracy respectively. Figure (a) shows the simulated spectra and figure (b) shows the spectra with changed positions, intensities and half-widths as differences from the average simulation. Note that, the changes in line position are so small that they are difficult to see.

reasonable representation of the shape of the methane profile. Also, as the range of simulations encompassed the single maximum and minimum observed methane and water vapour concentrations and temperatures whilst the observation which are being simulated are the average for a three month period, it is inconceivable that the true profile required to accurately simulate that observed is outside of the range used in the sensitivity study. Therefore, the inability for GenIn2 to simulate the observed methane band must also be due to a deficiency in the model rather than its input profiles. The spectroscopy of the model is the most obvious candidate. The spectroscopy used to create these simulations was HITRAN2000 with updates to 2001.¹¹ For each line listed, HITRAN also includes uncertainty codes detailing the possible uncertainty in line position, intensity and the air broadening half-width. We investigate whether the range of uncertainty of the HITRAN parameters is large enough so that the observed spectrum is encompassed by the range of spectra simulated using the range of input profiles and the range of spectroscopic parameters.

Figure 7(a) shows 7 spectra all simulated using the average observed profiles (as detailed in the figure caption). The spectra shown as the solid black line was simulated using the published values in the HITRAN databases. The two spectra shown as the grey and black dashed lines were simulated with the line intensities in HITRAN changed to be the maximum and minimum values possible within the published uncertainty range. The two spectra shown as dotted lines were simulated using the line positions changed to their maximum and minimum positions within their published ranges and the spectra

shown as dot-dashed lines were simulated using the half widths changed to the maximum and minimum values within their published ranges. Figure 7(b) shows the same 6 spectra simulated with the altered HITRAN values as differences from the spectra simulated using the published HITRAN values. Note that, the uncertainty in the line positions is so small that the spectra with the altered line positions are indistinguishable from the simulation created using the published values.

It is clear that only a combination of the maximum uncertainties in both the line width and the air broadening half-width with the most extreme profiles of temperature, methane and water vapour would enable the range of simulated spectra to encompass that observed. This seems an unlikely solution particularly considering the poor match of the extreme profiles to the remainder of the spectrum outside the methane band. It is also worth noting that the size of the change in the spectrum due to uncertainty in HITRAN is only lightly dependent on the input profiles and so when a difference spectrum is considered, errors in HITRAN can not account for any of the inability to simulate the methane band. A model deficiency which is both larger and more highly dependent of the particular input profile is required to explain the observed inability to simulate the spectrum in the ν_4 methane band. A possible candidate is the omission of line mixing in the methane band in the model. The most apparent effect of line mixing, at atmospheric pressures, is a reduction in the absorption coefficient in the line wings. At the low spectral resolutions of this study where individual lines can not be distinguished, this would be manifested as a reduction in absorption throughout the band. Line mixing in CO_2 is included in the GenIn2 model and considerably increases the brightness temperatures simulated in the region of the methane band.¹⁷ No similar model exists for line mixing in methane but in recent years there has been discussion in the literature into the observation and simulation of line mixing in methane. Pieroni et al.¹⁸ state that the pressure in the troposphere and lower stratosphere is sufficient that line mixing is necessary to explain the spectral shape and the Voigt lineshape used in this study is inadequate. Thusfar, line mixing in the ν_3 band of the methane is the only band to have been simulated at atmospheric pressures, with the only simulations and observations in the ν_4 band being, so far, at pressure much greater than that of the atmosphere. Therefore, it is suggested that the effects of line mixing, which is dependent on the concentration of methane, may be the cause of the inability to accurately simulate the spectra recorded by IRIS, IMG and AIRS, as well as the differences between those spectra, in the ν_4 methane band. We assert that further studies of line mixing in the ν_4 band at atmospheric pressures are required to complete our understanding of the full nature of the change in the atmospheric spectrum over the past 35 years. The interesting positive-going brightness temperature feature observed in AIRS-IMG difference spectrum, which was not well represented in the simulation, was probably caused by an increase in atmospheric temperature between 1997 and 2003 rather than a decrease in methane concentration as the methane concentration measurements suggest a slight increase in concentration. Without an model which can represent the methane band accurately, the exact cause of this particularly interesting feature must remain an hypothesis only.

6. CONCLUSIONS

Three datasets of spectrally resolved OLR from IRIS, IMG and AIRS have been normalised to the specifications of IRIS and direct comparison of the change in the radiative forcing over the time period 1970 to 2003 has been achieved. The changes observed, with the exception of the ν_4 band of methane, have been shown to be in agreement, within the noise equivalent brightness temperature of the instruments, with that simulated using the known changes in atmospheric temperature and the greenhouse gases. The inability to accurately simulate the ν_4 methane band was discussed in depth. It was shown that the scaling of the US tropical atmospheric profile of methane with the average CMDL ground based flask measurements, as used in the simulations, was an accurate representation of the average observed methane profile. Comparisons of simulations created using MODTRAN and GenIn2 showed only small differences in the difference spectrum, but large difference in the absolute spectrum. A sensitivity study showed that, whilst MODTRAN was unable to simulate an average spectrum with a methane band as deep as that observed, GenIn2 overestimated the depth of the band. Uncertainty in the spectroscopy parameters, as published in the HITRAN database, was shown to be smaller than the size of the difference between the methane band observed and that simulated. Line mixing of methane was suggested as a possible candidate for the cause of the inability as preliminary studies of line mixing in methane at atmospheric pressure show a large effect.

ACKNOWLEDGMENTS

This work was supported by a NERC studentship. We thank L. Chen and R. Goody for providing access to the IRIS data and H. Kobayashi for providing access to the IMG data. AIRS data was provided by the GES DISC DAAC at <http://daac.gsfc.nasa.gov/atmodyn/airs>. CMDL gas concentration data provided by the Climate Monitoring and Diagnostics Laboratory, Boulder, Colorado, USA from their website at <http://www.cmdl.noaa.gov/>.

REFERENCES

1. J. E. Harries, H. E. Brindley, P. J. Sagoo, and R. J. Bantges, "Increases in greenhouse forcing inferred from the outgoing longwave radiation spectra of the Earth in 1970 and 1997," *Nature* **410**, pp. 355–357, 2001.
2. J. Griggs and J. Harries, "Comparison of spectrally resolved outgoing longwave radiation data between 1970 and present," in *Proceedings of SPIE*, 2004.
3. R. Hanel and B. Conrath, "Thermal emission spectra of the Earth and atmosphere from the Nimbus 4 michelson interferometer experiment," *Nature* **228**, pp. 143–145, 1970.
4. R. Hanel, B. Schlachman, D. Rogers, and D. Vanous, "Nimbus 4 michelson interferometer," *Applied Optics* **10**(6), pp. 1376–1382, 1971.
5. "IMG mission operation and verification committee," in *Interferometric Monitor for Greenhouse Gases*, H. Kobayashi, ed., IMG Project Technical Report, Central Research Institute of Electric Power Industry (CRIEPI) Komae Research Laboratory, Kamoe-shi, Tokyo, 1999.
6. H. Kobayashi, A. Shimota, C. Yoshigahara, I. Yoshida, Y. Uehara, and K. Kondo, "Satellite-borne high-resolution FTIR for lower atmosphere sounding and its evaluation," *IEEE Transactions on Geoscience and Remote Sensing* **37**(3), pp. 1496–1507, 1999.
7. H. H. Aumann and R. J. Pagano, "Atmospheric Infrared Sounder on the Earth Observing System," *Optical Engineering* **33**(3), pp. 776–784, 1994.
8. J. Griggs and J. Harries, "Comparison of the spectrally resolved outgoing longwave radiation between 1970 and 2003." submitted to *Journal of Climate*, 2005.
9. E. Dlugokencky, K. Masarie, P. Lang, and P. Tans, "Continuing decline in the growth rate of the atmospheric methane burden," *Nature* **393**, pp. 447–450, 1998.
10. G. Anderson, F. Kneizys, J. Chetwynd, J. Wang, M. Hoke, L. Rothman, L. M. Kimball, R. McClatchey, E. Shettle, S. Clough, W. Gallery, L. Abreu, and J. Selby, "FASCOD/LOWTRAN: Past/present/future," in *18th Annual Review Conference on Atmospheric Transmission Models, 6-8 June 1995*, 1995.
11. L. Rothman, A. Barbe, D. C. Benner, L. Brown, C. Camy-Peyret, M. Carleer, K. Chance, C. Clerbaux, V. Dana, V. Devi, A. Fayt, J.-M. Flaud, R. Gamache, A. Goldman, D. Jacquemart, K. Jucks, W. Lafferty, J.-Y. Mandin, S. Massie, V. Nemtchinov, D. Newnham, A. Perrin, C. Rinsland, J. Schroeder, K. Smith, M. Smith, K. Tang, R. Toth, J. V. Auwera, P. Varanasi, and K. Yoshino, "The HITRAN molecular spectroscopic database: Edition of 2000 including updates through 2001," *Journal of Quantitative Spectroscopy and Radiative Transfer* **82**, pp. 5–44, 2003. doi:10.1016/S0022-4073(03)00146-8.
12. G. Anderson, S. Clough, F. Kneizys, J. Chetwynd, and E. Shettle, *AFGL Atmospheric Constituent Profiles (0-120km)*, AFGL-TR-86-0110, AFGL (OPI), Hanscom AFB, MA 01736, 1986.
13. E. Dlugokencky, L. Steele, P. Lang, and K. Masarie, "Atmospheric methane at Mauna Loa and Barrow observatories: Presentation and analysis of in situ measurements," *Journal of Geophysical Research*, 1995.
14. J. Russell III, L. Gordley, J. Park, S. Drayson, D. Hesketh, R. Cicerone, A. Tuck, J. Frederick, J. Harries, and P. Crutzen, "The Halogen Occultation Experiment," *Journal of Geophysical Research* **98**(D6), pp. 10777–10797, 1993.
15. J.-M. Thériault, G. Anderson, J. Chetwynd, Y. Qu, E. Murphy, V. Turner, M. Cloutier, and A. Smith, "Retrieval of tropospheric profiles from IR emission spectra: Investigations with the double beam interferometer sounder (DBIS)," in *Optical Remote Sensing of the Atmosphere 1993 Technical Digest*, **5**, p. 78, (Opt. Soc. of Am., Washington, D.C.), 1993.
16. D. Edwards, *GENLN2: A general line-by-line atmospheric transmittance and radiance model*. NCAR Technical Note, NCAR/TN-367+STR, Boulder CO., 1992.
17. H. Brindley, *An investigation into the impact of greenhouse gas forcings on the terrestrial radiation field: Sensitivity studies at high spectral resolution*. PhD thesis, University of London, 1998.
18. D. Pieroni, J.-M. Hartmann, C. Camy-Peyret, P. Jeseck, and S. Payan, "Influence of line mixing on absorption by CH₄ in atmospheric balloon-borne spectra near 3.3 μm," *Journal of Quantitative Spectroscopy and Radiative Transfer* **68**, pp. 117–133, 2001.